Molecular Neurobiology (2023) 60:3464–3485
https://doi.org/10.1007/s12035-023-03261-7

Doublecortin-Expressing Neurons in Human Cerebral Cortex Layer II and Amygdala from Infancy to 100 Years Old

Ya-Nan Li[1] · Dan-Dan Hu[1] · Xiao-Lu Cai[1] · Yan Wang[1] · Chen Yang[1] · Juan Jiang[1] · Qi-Lei Zhang[1] · Tian Tu[1,2] · Xiao-Sheng Wang[1] · Hui Wang[1] · Ewen Tu[3] · Xiao-Ping Wang[4] · Aihua Pan[1] · Xiao-Xin Yan[1] · Lily Wan[1]

Received: 17 October 2022 / Accepted: 4 February 2023 / Published online: 6 March 2023

Abstract

A cohort of morphologically heterogenous doublecortin immunoreactive (DCX +) "immature neurons" has been identified in the cerebral cortex largely around layer II and the amygdala largely in the paralaminar nucleus (PLN) among various mammals. To gain a wide spatiotemporal view on these neurons in humans, we examined layer II and amygdalar DCX + neurons in the brains of infants to 100-year-old individuals. Layer II DCX + neurons occurred throughout the cerebrum in the infants/toddlers, mainly in the temporal lobe in the adolescents and adults, and only in the temporal cortex surrounding the amygdala in the elderly. Amygdalar DCX + neurons occurred in all age groups, localized primarily to the PLN, and reduced in number with age. The small-sized DCX + neurons were unipolar or bipolar, and formed migratory chains extending tangentially, obliquely, and inwardly in layers I–III in the cortex, and from the PLN to other nuclei in the amygdala. Morphologically mature-looking neurons had a relatively larger soma and weaker DCX reactivity. In contrast to the above, DCX + neurons in the hippocampal dentate gyrus were only detected in the infant cases in parallelly processed cerebral sections. The present study reveals a broader regional distribution of the cortical layer II DCX + neurons than previously documented in human cerebrum, especially during childhood and adolescence, while both layer II and amygdalar DCX + neurons persist in the temporal lobe lifelong. Layer II and amygdalar DCX + neurons may serve as an essential immature neuronal system to support functional network plasticity in human cerebrum in an age/region-dependent manner.

Keywords Adult neurogenesis · Brain evolution · Chain migration · Interneuron · Neuroplasticity

Introduction

A cohort of the so-called immature neurons has been reported in the cerebral cortex and amygdala in a growing list of adult and even old mammals, with their anatomical and functional implications remained incompletely understood [1–3]. The finding of these neurons could be tracked back for more than 30 years [4]. Thus, cells expressing the anti-apoptotic protein Bcl-2, polysialylated neural cell adhesion molecule (PSA-NCAM), and doublecortin (DCX) were initially reported in the piriform cortex in small rodents [5–9], and in the amygdala and adjoining cortex in nonhuman primates [7, 10–12]. Follow-up studies described these neurons in many mammalian species including humans [13–27]. These DCX + or alike neurons are now commonly referred to as layer II and amygdalar "immature" neurons that may play a critical role in support of cerebral structural plasticity [4, 28]. Indeed, layer II DCX + neurons show features of morphological

Ya-Nan Li and Dan-Dan Hu contribute equally to this work.

✉ Aihua Pan
panaihua@csu.edu.cn

✉ Lily Wan
wanll1203@csu.edu.cn

1 Department of Anatomy and Neurobiology, Central South University Xiangya Medical School, Changsha 410013, Hunan, China

2 Department of Neurology, Xiangya Hospital, Central South University, Changsha 410008, Hunan, China

3 Department of Neurology, Brain Hospital of Hunan Province, Changsha 410007, Hunan, China

4 Department of Psychiatry, The Second Xiangya Hospital, Central South University, Changsha 410031, Hunan, China

maturation and integration into functional neurocircuitry [13, 14, 29, 30], experience-related modulation [31–33], and aging or disease-related alterations [21, 34, 35]. Similarly, DCX + neurons in the amygdala are reportedly related to the evolutionary expansion and protracted development of this limbic structure in primates [36–39], as well as the pathogenesis of some neurological and neuropsychiatric disorders such as temporal lobe epilepsy, autism, and major depression [34, 36, 40, 41].

In humans, layer II DCX + neurons have been reported largely in the temporal lobe in adults [14, 21, 34, 42–44], and recently in the frontal and temporal lobes in infants [45–47]. Age-related changes of DCX + neurons in the human amygdala are shown among individuals from infancy up to 77 years old in a recent study [23]. A compelling question is whether, and if so, to what extent, layer II DCX + neurons would distribute over broader cerebral regions in humans during a certain period of postnatal life, as observed in some animal species [2, 4, 13, 14, 24]. Taking advantage of the progress with human brain banking [48, 49], we sought to determine the distribution and amount of cortical layer II and amygdalar DCX + neurons in human cerebrum throughout the lifespan in the current study. We also examined DCX + immature neurons in the hippocampal dentate gyrus (DG) and subventricular zone (SVZ) in the parallelly processed sections, which, if present, could provide an internal control for the specificity of the DCX antibody [9, 13, 16].

Materials and Methods

Human Brain Samples

Postmortem human brains were banked through a willed body donation program [48]. Informed consent for whole body donation was obtained from the donors or next-of-kin in compliance with the regulations set by Chinese government. A total of 35 brains from donors died at different ages and with relatively short postmortem delays (2–12 h) were used in this study. Based on donor's ages and in reference to the regional distribution pattern of layer II DCX + neurons observed in the brain sections, we arranged the cases into the infant/toddler, adolescent, adult, and aged groups (Table 1). All methods involving the handling, processing, and pathological evaluation of postmortem human brain materials were carried out according to a standard protocol of brain banking in China [50]. All brains in the aged group and some in the adult group (≥ 30 years old, y) were evaluated for AD-type pathologies as detailed in our recent studies [51–53]. All experimental protocols were approved by the Ethics Committee of Central South University Xiangya School of Medicine.

Tissue Preparation

Brains were bisected following removal from the skull, with one hemi-brain (ipsilateral to hand-dominant side) cut into ~ 1-cm-thick coronal slices and fresh-frozen at − 70 °C, and the other hemi-brain fixed in formalin for 2 weeks. The fixed half-brains were then cut coronally into 1-cm-thick slices. Blocks were prepared from the frontal, temporal, and occipital pole slices, from the frontal lobe slice passing the anterior end of the lateral ventricle, the temporal lobe slices at mid-hippocampal and mid-amygdalar levels, and the occipital lobe slice passing the posterior end of the lateral ventricle. These fixed brain blocks were cryoprotected in 30% sucrose in 0.1 M phosphate buffer, and then cut in a cryostat at 35-μm thickness. Sections from each block were collected orderly into 24 wells in culture plates in phosphate-buffered saline (PBS, 0.01 M, pH7.2), rinsed with PBS to remove the embedding medium, and then stored in a cryoprotectant (30% sucrose, 1% polyvinyl-pyrrolidone, and 30% ethylene glycol in 0.1 M phosphate buffer) at − 20 °C before they were used for immunohistochemistry. In addition, a number of brains were selected from the youth, adult, and aged groups (as indicated in Table 1), with tissue blocks in the temporal lobe dissected out from the frozen hemisphere, and processed for Western blotting.

Immunohistochemistry

For each immunohistochemical experiment, 3–4 equally spaced sections per region/brain from 4–5 samples were taken out from the cryoprotectant storage and rinsed with PBS three times at room temperature. The sections were then treated in PBS with 5% H_2O_2 for 30 min, and in PBS with 5% normal horse serum, and 0.3% Triton X-100 for 1 h at room temperature. Sections were reacted with a goat anti-DCX antibody (1:1000, sc-8066, Santa Cruz Biotech, CA, USA) overnight at 4 °C [13, 14, 16, 24], further with biotinylated universal secondary antibody at 1:400 (Vector Laboratories, Burlingame, CA) for 2 h, and with the avidin–biotin complex (ABC) at 1:400 (Vector Laboratories, Burlingame, CA) for 1 h. Immunoreaction product was developed in PBS with 0.003% H_2O_2 and 0.05% diaminobenzidine (DAB). Three 10-min washes with PBS were used between incubations. Sections were mounted on slides, counterstained with hematoxylin in subsets of sections, air-dried, and then coverslipped following dehydration and clearance.

Western Blot

The frozen temporal lobe slice at the level of the amygdala was identified from a given brain to obtain samples for Western blotting. A block from the superficial part of

Table 1 Demographic information of brain donors and application of postmortem brain samples

Group	Case#	Age	Sex	Clinical diagnosis and cause of death	Postmortem delay (hours)	Thal Aβ and Braak NFT staging	Sample usage
Infant and toddler ($n=6$)	1	6 m	M	Sudden infant death	4	N.A	IHC/CC
	2	8 m	M	Congenital bile duct occlusion	4	N.A	IHC/CC
	3	10 m	F	Pneumonia	3	N.A	IHC/CC
	4	1 y	F	Leukemia	5	N.A	IHC/CC
	5	2 y	M	Bile duct blockage	8	N.A	IHC/CC
	6	3 y	F	Mental retardation	12	N.A	IHC/CC
Adolescent ($n=8$)	7	10 y	M	Leukemia	12	N.A	IHC
	8	12 y	M	Cerebral palsy, epilepsy	6	N.A	IHC/CC/WB
	9	12 y	F	Thalassemia	12	N.A	IHC
	10	14 y	F	Tuberculosis	10	N.A	IHC/CC/WB
	11	16 y	F	Down syndrome	4	N.A	IHC/CC/WB
	12	16 y	F	Transposition of the great arteries	8	N.A	IHC/CC
	13	17 y	M	Acute leukemia	5	N.A	IHC/CC/WB
	14	18 y	M	Accident death	5	N.A	IHC/CC/WB
Adult ($n=10$)	15	22 y	F	Osteosarcoma	10	N.A	IHC
	16	28 y	M	Lung cancer	2	N.A	IHC/CC/WB
	17	29 y	F	Gastric cancer	6	N.A	IHC/CC/WB
	18	31 y	F	Leukemia	10	N.A	IHC/CC
	19	33 y	F	Dilated cardiomyopathy	12	0/0	IHC/CC
	20	38 y	M	Lung cancer	8	0/0	IHC/WB
	21	49 y	M	Leukemia	10	0/0	IHC/CC
	22	50 y	F	Vaginal cancer	8	0/0	IHC/CC/WB
	23	54 y	M	Liver cancer	7	0/0	IHC/WB
	24	56 y	M	Lung cancer	12	0/0	IHC
Aged ($n=11$)	25	65	M	Esophageal cancer	3	0/0	IHC/WB
	26	66	M	Cerebral stroke	5	0/0	IHC
	27	68 y	F	Breast cancer	4	0/0	IHC/CC
	28	71 y	M	Pulmonary heart disease	6	0/0	IHC/CC/WB
	29	74 y	M	Lung infection	5	0/III	IHC/CC/WB
	30	76 y	M	Myocardial infarction	7	0/III	IHC/CC/WB
	31	85 y	M	Glioma	12	2/IV	IHC/CC
	32	88 y	F	Multisystem failure*	9	4/V	IHC/CC
	33	91 y	M	Multisystem failure*	12	5/VI	IHC/CC/WB
	34	99 y	F	Cerebral stroke*	5	4/V	IHC
	35	101 y	M	Multisystem failure	4.5	4/V	IHC

Abbreviations: m month old; *y* year old; *N.A.* not assessed; *CC* cell count; *IHC* immunohistochemistry; *WB* Western blot; *0–5* phases of plaque pathology according to β-amyloid (Aβ) immunolabeling; *0–VI* stages of neurofibrillary tangles (NFTs) according to phosphorylated tau immunolabeling; *demented according to enquiry from next-of-kin

the temporal cortex and a block of the amygdala tissue near the lateral ventricle were dissected out from each slice, respectively. Frozen samples were homogenized on ice by sonication in T-PER extraction buffer (Pierce, Rockford, IL, USA) containing protease inhibitors (Roche, Indianapolis, IN, USA). Extracts were centrifuged at 15,000 g at 4 °C, with supernatants collected and protein concentrations measured by DC protein assay (Bio-Rad Laboratories, Hercules, CA, USA). Lysates containing equal amount of total protein loading were separated in SDS–polyacrylamide gels by electrophoresis, and electrotransferred to Trans-Blot pure nitrocellulose membranes. Membrane strips were incubated with antibodies to DCX (1:2000) and glyceraldehyde-3-phosphate dehydrogenase (mouse anti-GAPDH; 1:5000, Millipore Shanghai Trading Company Ltd., Shanghai,

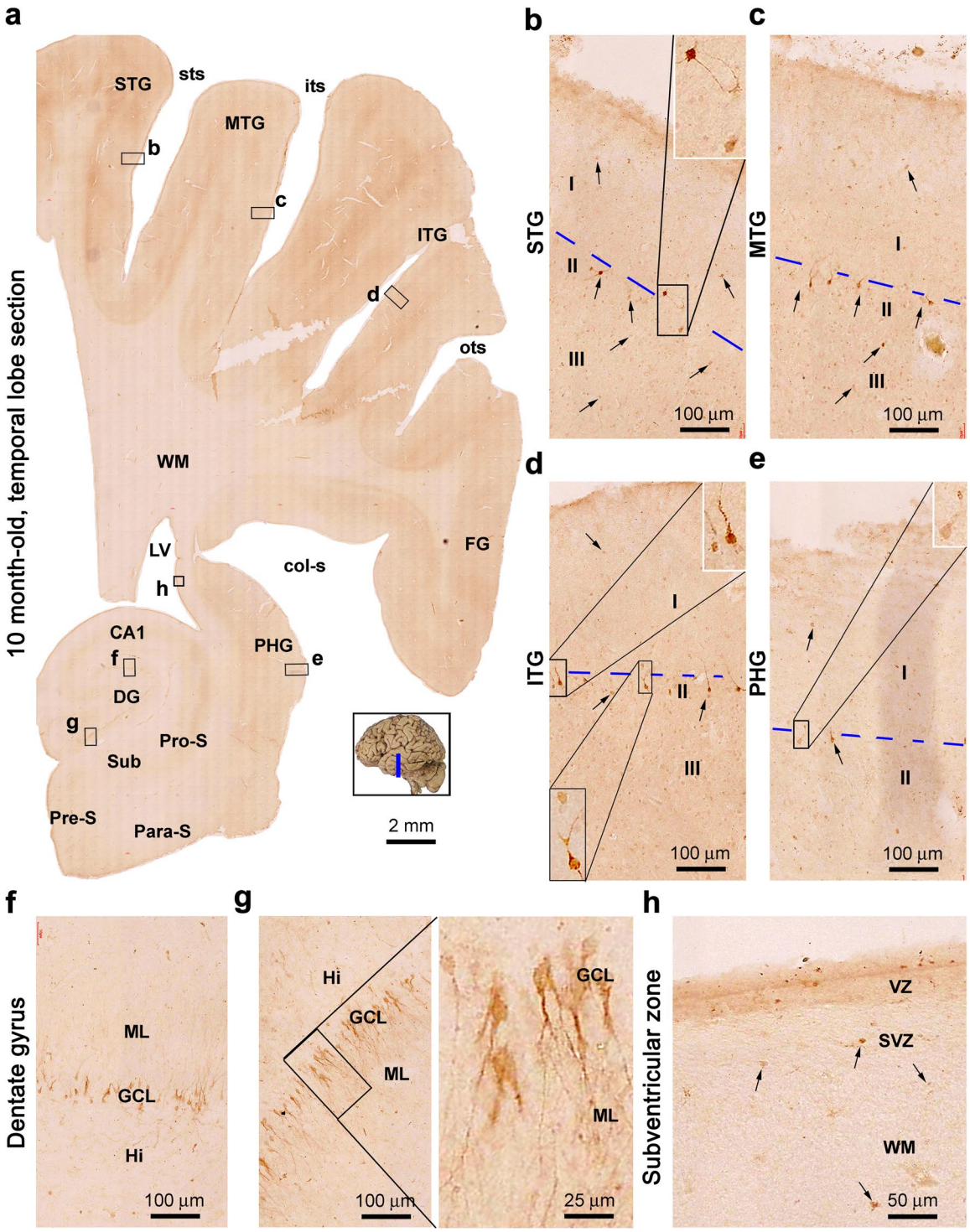

China). HRP-conjugated IgGs (rabbit anti-goat and anti-mouse, 1:10,000; Bio-Rad Laboratories, Hercules, CA, USA) and ECL-plus Western blotting substrate detection kit (Thermo Fisher Scientific; Waltham, MA, USA) were used to visualize the blotted protein bands. Western blotting images were documented with the UVP ChemStudio/PLUS device (Analytik Jena/UVP, USA).

Imaging, Quantification, Data Analysis and Figure Preparation

Sections with DAB immunolabeling were examined first on an Olympus BX51 microscope (cellSens Standard, Olympus Corporation, Japan) to assess the labeling quality and overall distribution pattern of labeled cells. All sections were

◂**Fig. 1** Doublecortin immunoreactive (DCX +) neuronal profiles in a temporal lobe section at the mid-hippocampal level from the brain of a 10-month (mo)-old infant. **a** Low-magnification Motic-scanned image, with framed areas enlarged as other panels as well as inserts as indicated. DCX + neuronal somata together with dendrite-like processes are found in all neocortical and entorhinal gyri, with the most distinct ones (as pointed by arrows) located at the border between layers I and II (**a**–**e**). A large number of labeled neurons are present in the hippocampal dente gyrus (DG) along the subgranular zone (SGZ), with their dendritic processes extending across the granule cell layer (GCL) into the molecular layer (ML) (**a**, **f**, **g**). A few DCX + cells are found at the subventricular zone (SVZ) surrounding the lateral ventricle (LV) (**h**). Blue broken lines mark the border of layers I and II. Additional abbreviations: STG, superior temporal gyrus; sts, superior temporal sulcus; MTG, middle temporal gyrus; ITG, inferior temporal gyrus; its, inferior temporal sulcus; ots, occipitotemporal sulcus; FG, fusiform gyrus; col-s, collateral sulcus; PHG, parahippocampal gyrus; CA1, hippocampal CA1 sector; Pro-S, prosubiculum; Sub, subiculum; Pre-S, presubiculum; Para-S, parasubiculum; Hi, hilus; WM, white matter. I, II, and III: cortical layers. VZ: ventricular zone. Scale bars are as indicated in each panel

then scan-imaged using the 40 × objective on an automated Motic-Olympus microscope (Motic China Group Co. Ltd., Wuhan, Hubei, China). The distribution and morphology of DCX + neurons were examined across the Motic images at different magnifications. The resulting digital images were used for on-screen examination and exporting of micrographs for figure presentation and cell count.

Hematoxylin-counterstained sections passing the frontal, temporal, and occipital poles, and at the mid-amygdalar and mid-hippocampal levels, respectively, were used to count the DCX + neurons on the Motic imaging analysis interface using a randomized sampling approach [24]. The counting zones consisted of 200 μm × 200 μm grids were randomly generalized and tagged in reference to the scales on the X and Y axes over the section area. We quantified DCX + neurons over layer II along the gyral portions of the neocortex, PLN of the amygdalar complex, and the granule cell layer (GCL) to subgranular zone SGZ of DG. The mean densities of DCX + neurons (number of cells/μm^2) in a given region were calculated based on the data obtained from two sections from each brain. The cell density data were recorded for the age groups. Because there was age-related loss of DCX + neurons in particular brain regions, a zero value was given in such cases to allow statistical analysis and graphing.

The cell counting data were arranged according to the age groups, with means and S.D. calculated for the groups and analyzed statistically using one-way ANOVA with Bonferroni's Multiple Comparison Test (GraphPad Prism 5.1, San Diego, CA, USA). Immunoblot images were quantified using the OptiQuant software, with the optic density (o.d.) over blotted DCX protein bands obtained, followed by a normalization to the levels of GAPDH in the same lysates. P value < 0.05 was set as the cutoff for significant difference between the means of comparing groups. Figures were assembled with Photoshop 7.1.

Results

Observation of Cortical and Amygdalar DCX + Neurons in the Infant/Toddler Cases

We observed DCX + cells in all the sections from the cases in the infant/toddler group (Table 1). Thus, DCX + cells were present in the cortex in the sections from all cerebral lobes, in the amygdalar complex, as well as in the dentate gyrus. The morphological features of DCX + neurons are described below, with representative images illustrated (Figs. 1, 2, 3, 4, 5; Suppl Fig. 1).

As seen in the temporal lobe section at the mid-hippocampal level from the 10-month-old infant, DCX + cells occurred in the superficial layers of the neocortical (Fig. 1a–d) and the entorhinal (Fig. 1a, e) regions. The cells were mostly distributed in layer II, with variable morphology and labeling intensity. The most distinctly stained ones were smaller in size with a unipolar or bipolar soma, while those in larger sizes were often multipolar and stained lighter. Lightly stained DCX + cells were also seen in layer I, and III to IV, besides II (Fig. 1b–e). In the DG, a large number of DCX + cells occurred along the SVZ and the lower portion of GCL. Their dendritic processes extended into and across the molecular layer (ML) (Fig. 1a, f, g). A few DCX + cells were present in the SVZ around the lateral ventricle (Fig. 1a, h).

In the temporal lobe section passing the amygdala, DCX + neurons were packed in the PLN (Fig. 2a, b). They were mostly small in size with moderate labeling intensity and had few or very short processes. Some DCX + cells in the PLN arranged as migratory chains extending towards and into the basolateral (BL) and basomedial (BM) nuclei (Fig. 2b). Moderately and lightly stained DCX + neurons were observed in all amygdalar subnuclei (Fig. 2b). In the temporal neocortex (Fig. 2c, d) and entorhinal cortex (Fig. 2e), DCX + neurons varying in somal size and labeling intensity were fairly abundantly present. Again, they occurred mostly in layer II, but were also seen in layers I, III, and even IV (Fig. 2d–e). A widespread cerebral distribution of cortical DCX + neurons could be realized by examining the sections from this brain passing the frontal, temporal, and occipital poles (Fig. 3a–c). In all of these sections, the strongly labeled DCX + neurons consistently occurred around layer II, some arranged in chains extending tangential or oblique relative to the pial surface. Moderately and lightly stained DCX + cells were seen across layers I to III (Fig. 3a1–a3, b1–b3, c1–c3).

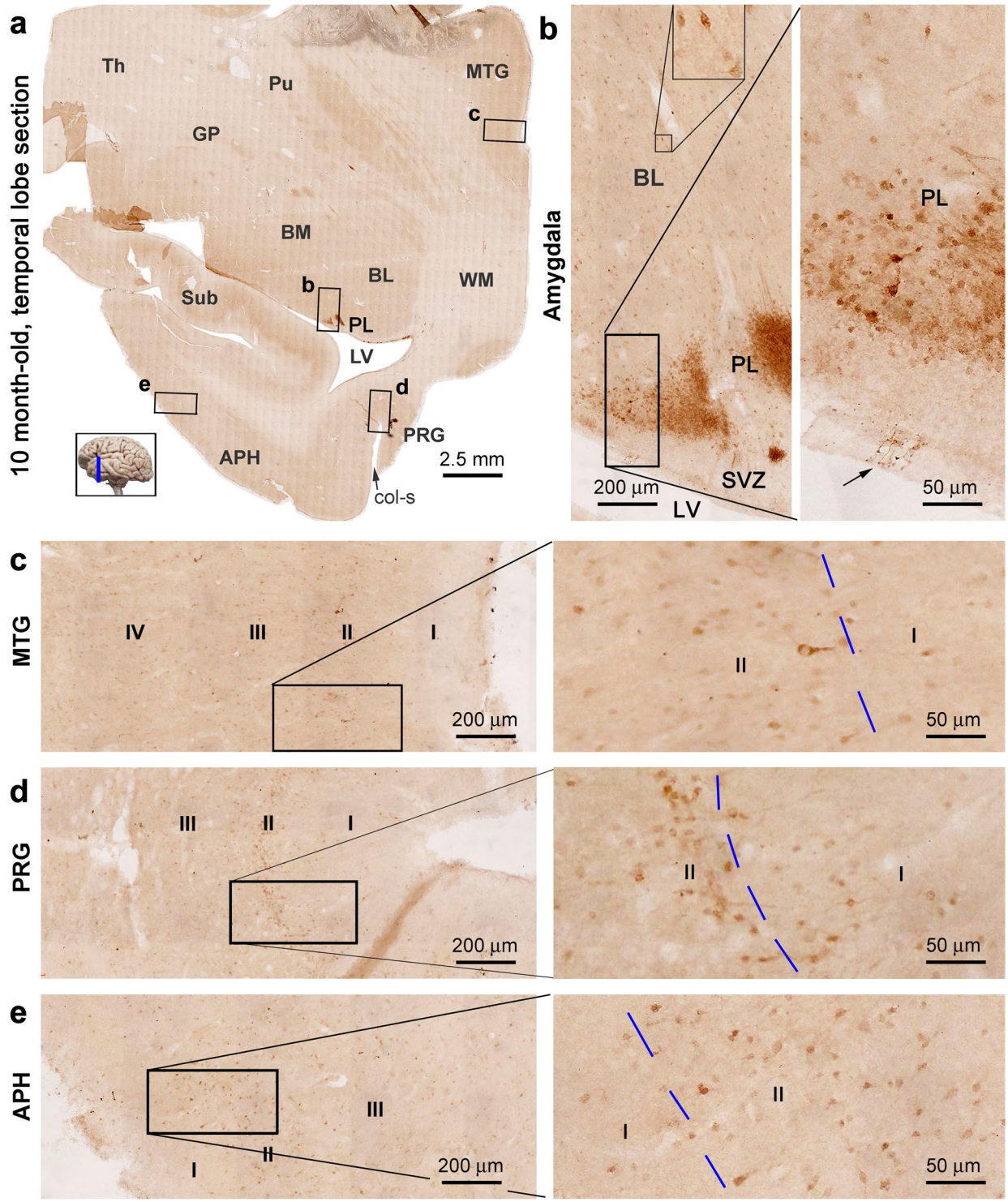

Fig. 2 DCX + neuronal profiles in a temporal lobe section at the amygdalar level from the 10 month-old old infant brain. **a** Low-magnification image, with framed areas of the neo- and palo-cortices, and the amygdala enlarged as indicated (**b**–**e**). DCX + cells are densely packed at the paralaminar (PL) nucleus (PLN) of the amygdalar complex, while lightly to moderately stained cells existed in all other subdivisions (**b**). There are groups (pointed by an arrow) of labeled cells at the subventricular zone (SVZ), which are separated from those in the PLN by a zone without labeled cells (**b**). A cellular band is seen over the superficial cortical layers, which contain DCX + cells with light to strong reactivity and heterogenous morphology (**c**–**e**). The most strongly labeled cells occur in layer II especially around its border to layer I in all cortical areas. Blue broken lines mark the border of layers I and II. Th, thalamus; Pu, putamen; GP, globous pallidum; BM, basomedial nucleus; BL, basolateral nucleus; APH, anterior parahippocampal gyrus; PRG, perirhinal gyrus. Other abbreviations are as defined in Fig. 1, and scale bars are as indicated

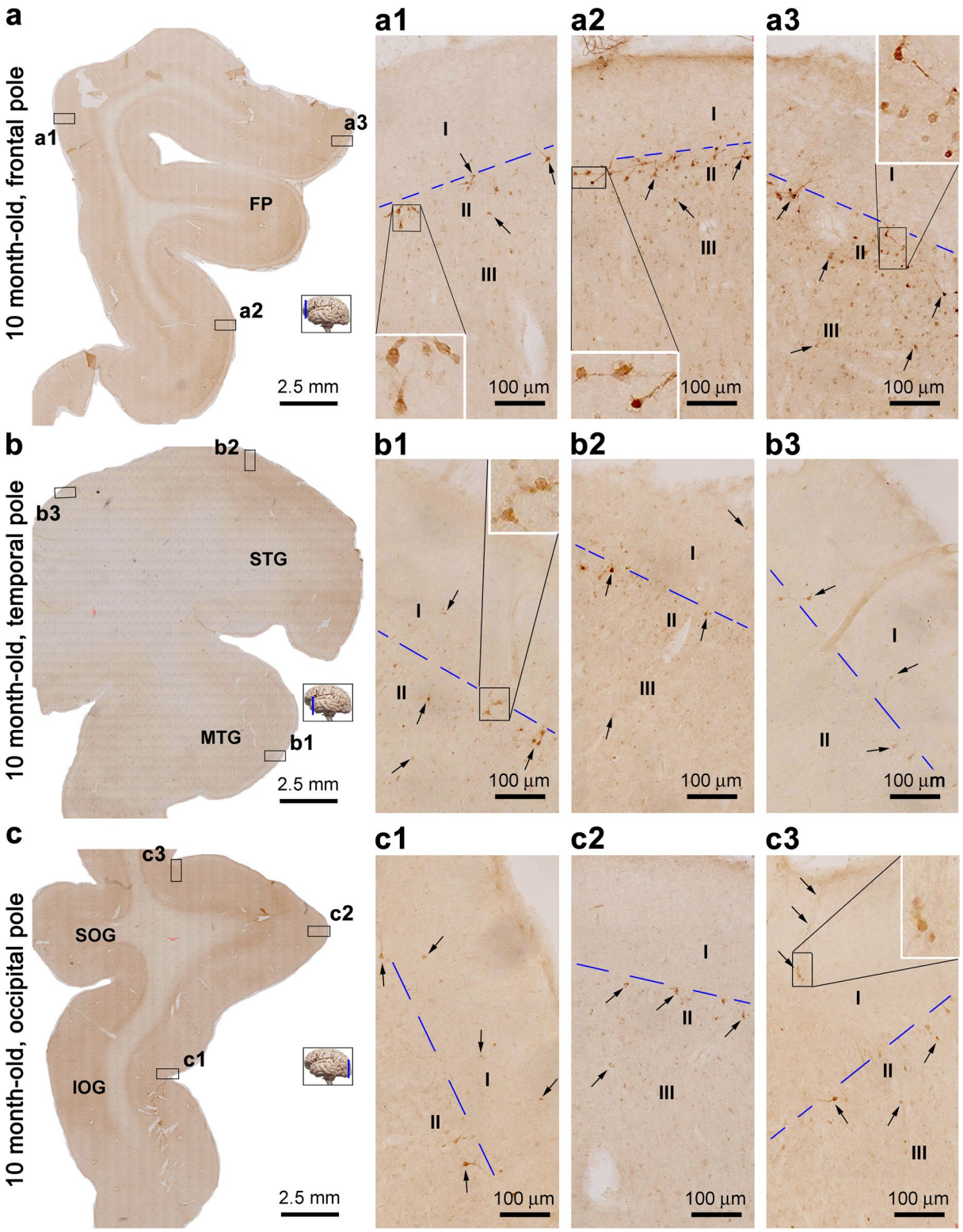

Fig. 3 DCX + neuronal profiles in the neocortex of the frontal, temporal, and occipital poles in the 10-month-old old infant brain. **a–c** Low-magnification views with boxed areas enlarged as the corresponding panels and inserts as indicated. Strongly labeled neuronal somata with dendrite-like processes (examples are pointed by arrows) are present along the border between layers I and II in all enlarged image panels. Lightly stained neuronal somata are seen over layers I, III, and IV (examples are pointed by arrows), besides II, by closer examination. Blue broken lines mark the border of layers I and II. FP, frontal pole; STG, superior temporal gyrus; MTG, middle temporal gyrus; SOG, superior occipital gyrus; IOG, inferior occipital gyrus; I–IV, cortical layers. Scale bars are as indicated

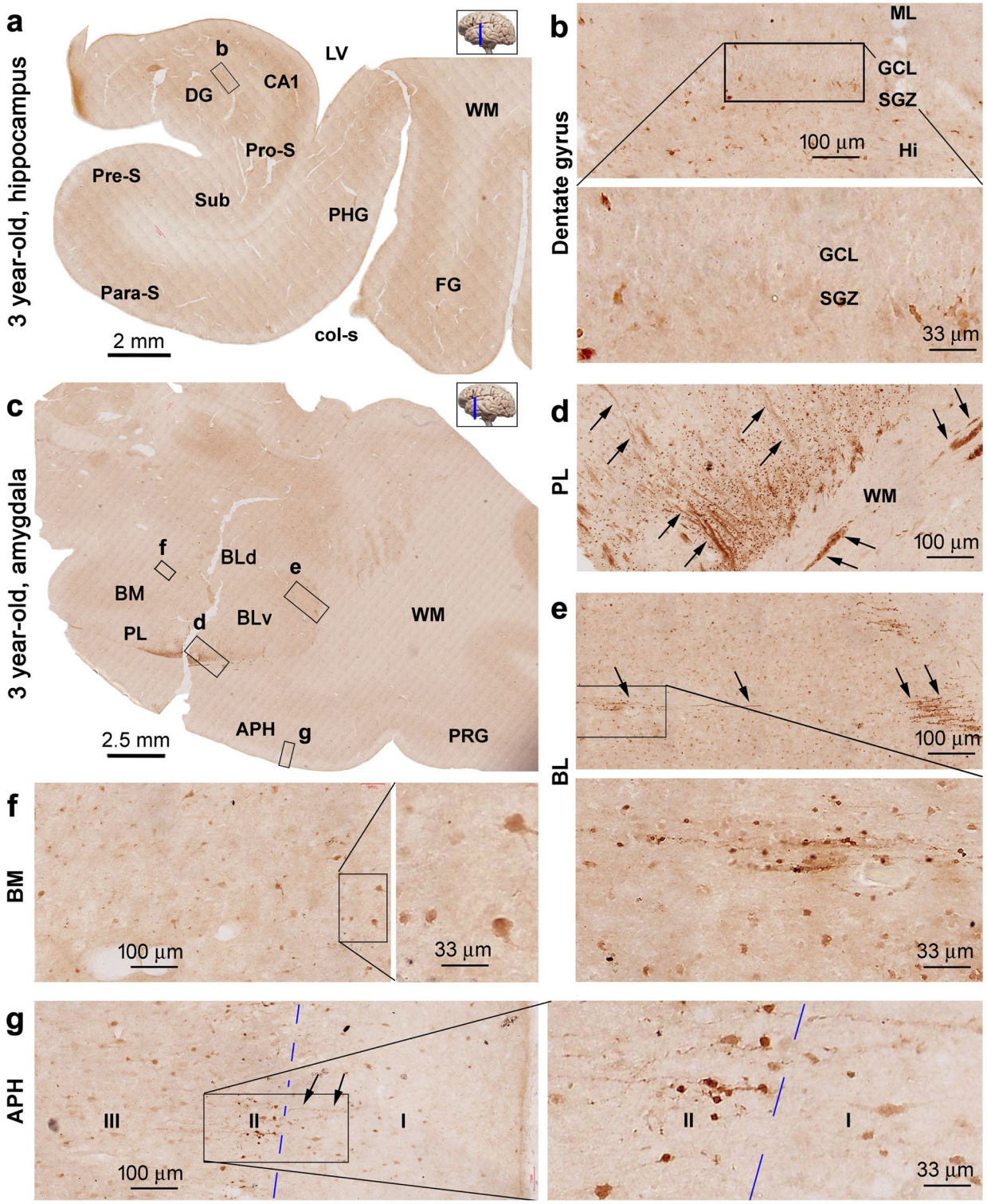

Fig. 4 Images showing DCX + neuronal profiles in the temporal lobe structures in the 3-year-old case. Labeled neuronal profiles are illustrated in low- and high-magnification images from sections at the levels of the hippocampus and amygdala as indicated. A small population of DCX + are seem in the dentate gyrus (DG) along the subgranular zone (SGZ) and in the hilus (Hi) (**a**, **b**). In the amygdala (C), DCX + cells are tightly packed in the paralaminar (PL) nucleus, but also seen in the basolateral (BL), and basomedial (BM) nuclei (**c**–**f**), with migratory cellular chains extending from the PL into other subnuclei (**d**–**f**). (**g**) shows DCX + cortical neurons in the anterior parahippocampal gyrus (APH), with the small-sized and heavily labeled ones arranged in chains (pointed by arrows) extending from layer I into II/III. Blue broken lines mark the border of layers I and II. Abbreviations are as defined in Figs. 1 and 2. Scale bars are as indicated

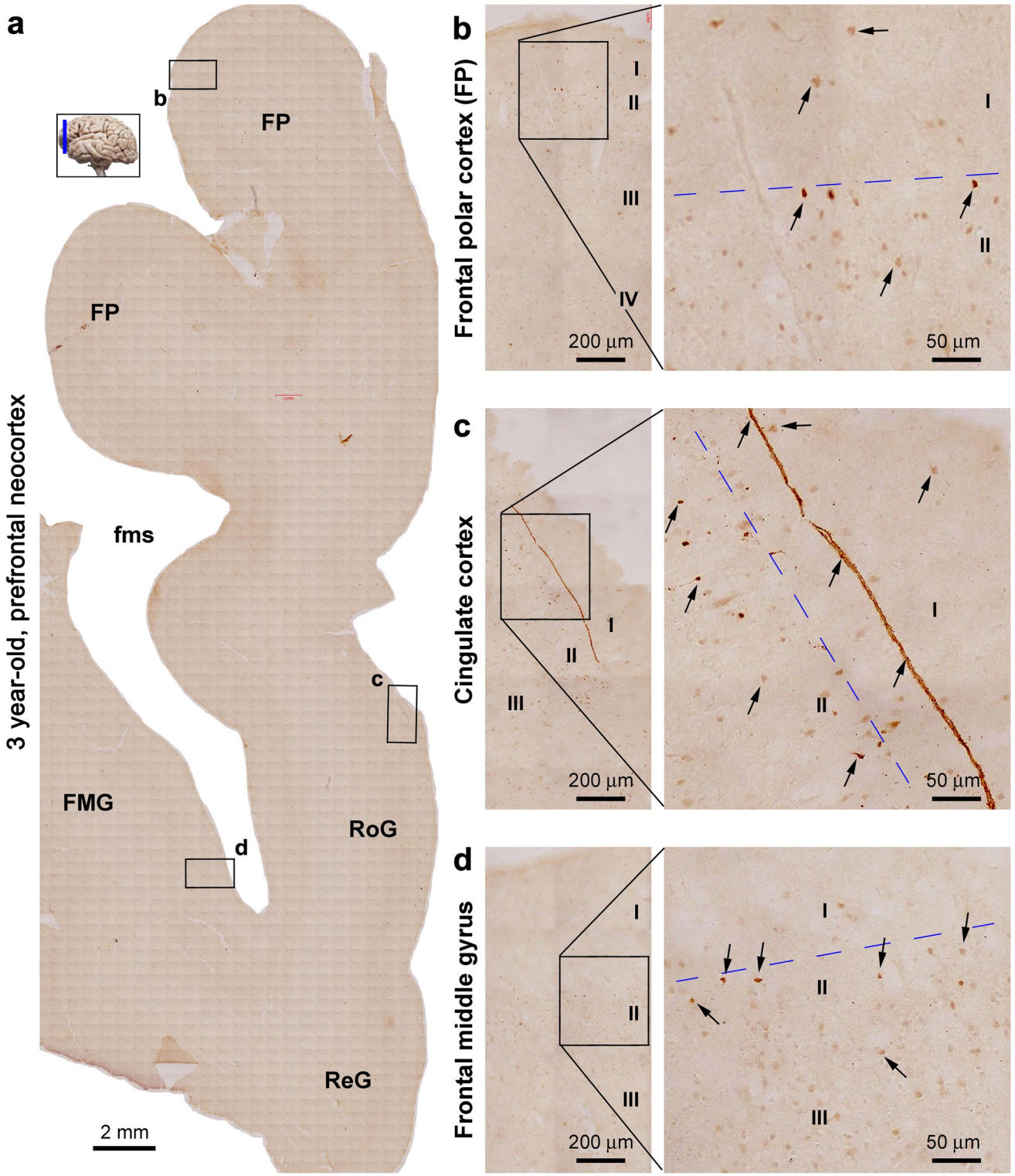

Fig. 5 DCX + neuronal profiles in the frontal pole cortical areas in the 3 year-old case. **a** Motic image at low magnification, with the framed areas enlarged to illustrate the labeling in the frontal pole (**b**), cingulate (**c**), and frontal middle (**d**) gyri, respectively. Labeled neuronal profiles are found in layers I–IV, including a small subpopulation of small-sized cells in layer II (as pointed by arrows). A very long migratory chain runs tangentially along layer I in (**c**, arrows). Blue broken lines mark the border between layers I and II. FP, frontal pole; FMG, frontal middle gyrus; fms, frontomarginal sulcus; RoG, rostral gyrus; ReG, gyrus rectus; I–IV, cortical layers. Scale bars are as indicated

As with the above case, a large number of DCX + neurons were found in various cerebral region in the 1-year-old case, as shown in a temporal lobe section for example (Suppl. Figure 1). In the brain of the 3-year-old case (Fig. 4), the overall regional distribution of cortical and amygdalar DCX + cells were similar to that seen in the infant brains. However, there was an apparent reduction in the number of subgranular DCX + cells in the DG in this case (Fig. 4a, b). Thus, DCX + cells were located discretely in the SGZ and the hilus, with a few in the middle and upper tiers of the GCL (Fig. 4b). The dendritic arbors of these immature granule cells were also less prominent than those seen in the infant brains (Fig. 1f, g; Suppl. Figure 1e). In the section passing the amygdala, strongly labeled DCX + cells were densely packed across the PLN, along with many migratory chains (Fig. 4c–e, pointed by arrows). The cellular density tended to reduce as moving into the central areas of the amygdalar complex, with labeled somata and processes also formed migratory chains (Fig. 4d–f). Moderately and lightly stained DCX + cells were present in the BM and BL, along with a small number of migratory cellular chains (Fig. 4e, f). There were also several migratory chains running tangentially in the white matter of entorhinal cortex (Fig. 4c, d). The laminar distribution and morphology of DCX + cells in the temporal neocortex and entorhinal cortex in this case were comparable to that seen in the infants described above, including some migratory chains extending from layer I into layers II and III (Fig. 4g). Furthermore, a pan-cerebral distribution of the layer II DCX + neurons persisted in this case, as shown in a section passing the frontal pole for example (Fig. 5). Again, heavily stained DCX + neurons in relatively small somal sizes occurred around II, while lightly to moderately stained cells in larger somal sizes were found from layers I–IV (Fig. 5a–d). A few tangential DCX + chains were observed in layer I, which could extend up to several hundred microns (Fig. 5a, c).

Observation of Cortical and Amygdalar DCX + Cells in the Adolescent Cases

Data from donors aged from 10–18 years were included in this group (Table 1). In these cases, there were fewer DCX + neurons in the superficial cortical layers relative to the infant/toddler cases. Thus, the labeled cells remained detectable in the sections from the frontal, parietal, and occipital lobes, while a significant population existed in the cortex essentially across the entire temporal lobe subregions. In general, DCX + cells in the DG became rarely detectable. In contrast, DCX + cells were consistently present in the amygdalar regions. Images from a 16-year-old case (#12 in Table 1) are included as examples to illustrate the distribution and morphology of cortical and amygdalar DCX + neurons (Figs. 6 and 7).

As seen in the temporal lobe section passing the mid-hippocampus, many DCX + neurons were observed in layers I–IV in the neocortical and entorhinal cortical regions, with the heavily labeled neurons localized to layer II, and lightly to moderately labeled ones present in layers I–IV (Fig. 6a–d). The strongly labeled neurons sometimes occurred in chains oriented perpendicularly to the pial surface (Fig. 6b-d, pointed by arrows). Moving down into the hippocampal formation, DCX + neurons could not be found in the DG (Fig. 6a, e). In the temporal lobe section passing the amygdala (Fig. 7a), a band of strongly labeled DCX + cells occurred deep to layer I in the neocortical and entorhinal areas (Fig. 7a, b). Most cells were associated with migratory chains arranged in a "waterfall-like" pattern extending from layer I into II/III (Fig. 7b, pointed by arrows). Lightly to moderately stained DCX + cells were present across layer I to IV. In the amygdala, a large number of labeled neurons occurred around PLN, while many neurons were also found as moving into to other subnuclei (Fig. 7a, c, d). The cells with heavy immunoreactivity were largely bipolar, with some associated with migratory chains from PLN into other nuclei (Fig. 7c, d). In the section passing the temporal pole (Fig. 7e), there existed a substantial amount of DCX + cells forming a band over layer II across the gyral and sulcal cortical regions (Fig. 7f, g). These DCX + neurons were also morphologically heterogenous, with some arranged as inwardly oriented migratory chains (Fig. 7f, g).

Observation of Cortical and Amygdalar DCX + Cells in the Adult Cases

Brains from donors at ages from 22–56 years were examined in this group (Table 1). Overall, DCX + cortical neurons were occasionally found in the frontal, parietal and occipital lobe sections, but consistently seen in the cortex across the temporal lobe, although with a reduced amount relative to the adolescent cases. DCX + neurons were clearly found in the amygdala. In contrast, DCX + neurons were rarely identified in the DG (data not shown). Representative images from two cases (38 and 50 years old) are shown to illustrate the DCX + neurons.

As seen in the section passing the mid-hippocampus from the 38-year-old case (Fig. 8), a small group of cortical DCX + cells were found in layers I–III in the neocortical areas. Thus, in the precentral neocortex (Fig. 8a, b), most cells were relatively large and lightly to moderately stained, while a few small-sized ones also present (pointed by arrow, Fig. 8b). In the temporal neocortex and entorhinal cortex in the 38- and 50-year-old cases, many small-sized bipolar neurons were found in the superior, middle, and inferior temporal gyri (STG, MTG and ITG), fusiform gyrus (FG), and parahippocampal gyrus (PHG), some arranged in chains or

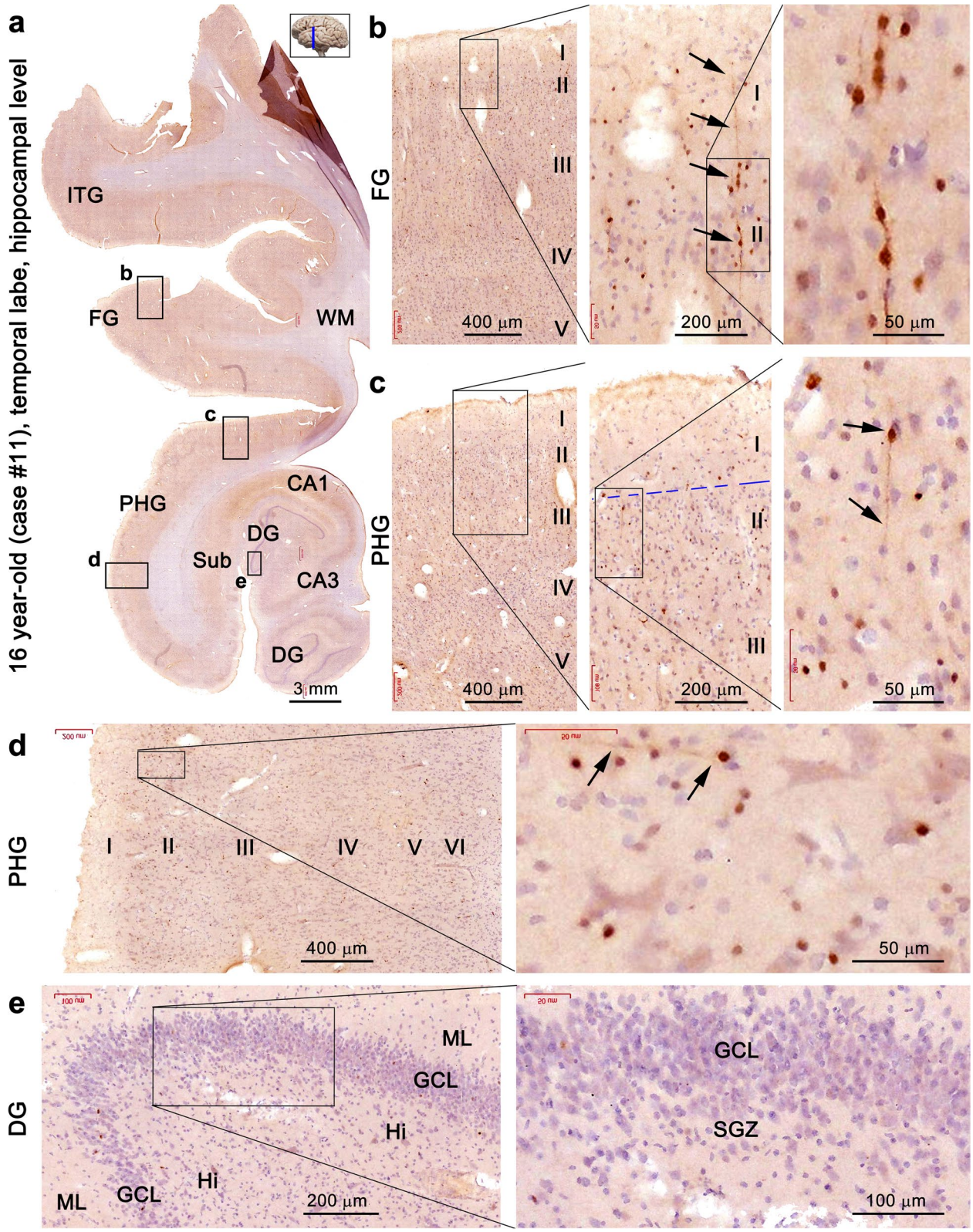

Fig. 6 DCX + neuronal profiles in a temporal lobe section at the mid-hippocampal level from the 16-year-old case. The section is counter-stained with hematoxylin. **a** shows the lower power view, with framed areas enlarged sequentially. **b**–**d** show DCX + cells in the neocortex. Note the inwardly arranged chains from layer I to II/III (pointed by arrows). DCX + neurons are not visible in the dentate gyrus (DG) (**e**). Blue broken lines mark the border of layers I and II. Abbreviations are as defined in Fig. 1, and scale bars are as indicated

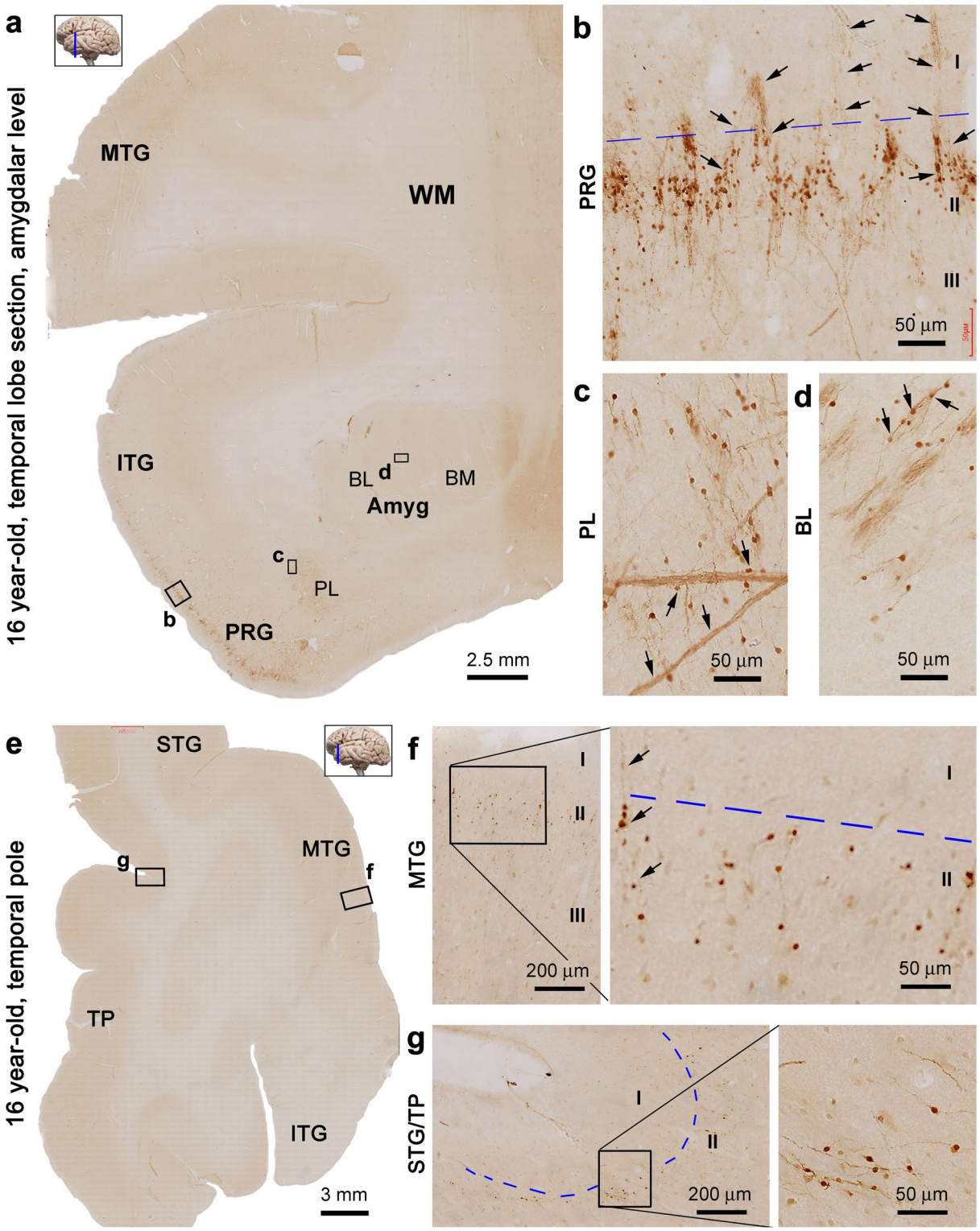

Fig. 7 DCX + neuronal profiles in temporal lobe subregions in the 16-year-old case. **a**, **e** show the low-magnification views of the sections at the levels of the amygdala and temporal pole, with the boxed areas enlarged as indicated. **b** shows labeled cells and migratory structures in the perirhinal gyrus (PRG); note the inwardly oriented chains from layers I to III (pointed by arrows). **c** shows labeled cells and migratory chains in the paralaminar (PL) and basolateral (BL) nuclei of the amygdala. **f**, **g** show the labeled neuronal profiles in temporal pole neocortex. Additional abbreviations are as defined in Figs. 1 and 2. Blue broken lines mark the border of layers I and II. Scale bars are as provided in each panel

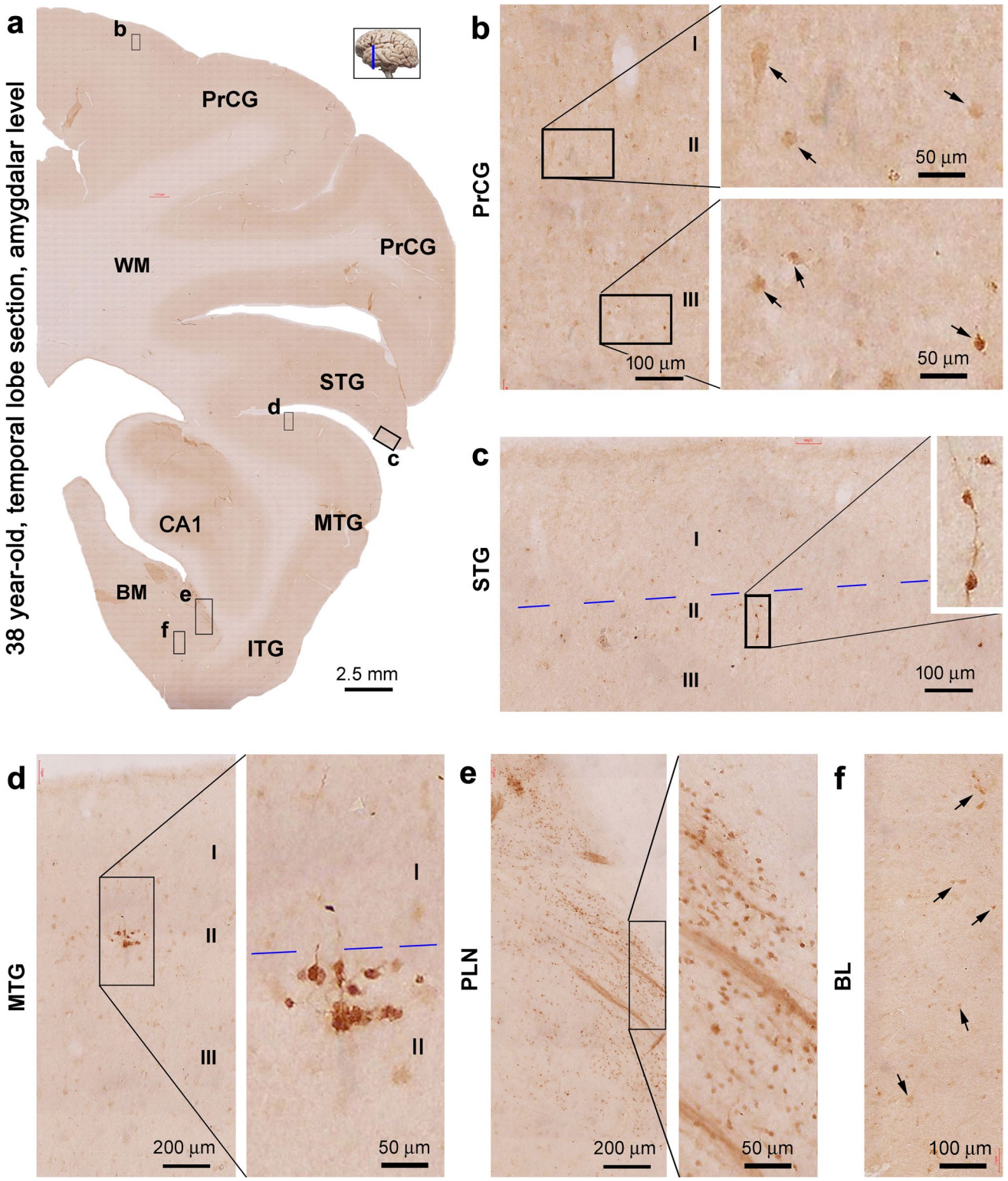

Fig. 8 DCX + neuronal profiles in the temporal lobe section at the level of amygdala in the 38-year-old case. Labeled neuronal profiles at different cortical and amygdalar locations (boxed areas in the low-magnification image) are enlarged as indicated (**a**). Labeled cells in the precentral gyrus (PrCG) are most lightly stained (**b**), whereas in the temporal neocortex, heavily stained neurons are also present around layer II (**c**, **d**). Labeled cells are densely packed at the amygdalar paralaminar (PL) nucleus, whereas the cells in the basolateral nucleus (BM) are mostly stained lightly (**f**). Additional abbreviations are as defined in Fig. 2. Scale bars are marked

clusters (Fig. 8c, d; Supp. Figure 2a–e; Suppl. Figure 3a–d). In the amygdala, a dense population of DCX + cells occurred at the PLN, with migratory chains also seen around this region (Fig. 8a, e; Supp. Figure 2d–f). In the BM and BL subdivisions, DCX + neurons were lightly and moderately stained in general, with a few heavily labeled cells (Fig. 8f; Supp. Figure 2f). No DCX + neuronal profiles could be identified in the DG, including at the SGZ (Suppl. Figure 3e).

Observation of Cortical and Amygdalar DCX + Neurons in the Aged Cases

Sections from donors at ages 68–101 years were analyzed in this group (Table 1). The DCX + neurons were essentially not detectable across the sections passing the frontal, parietal, and occipital pole. However, some labeled cells were still found in the neocortex and entorhinal cortex adjoining the amygdala. There was still a substantial number of DCX + neurons in the amygdala especially around the PLN. Again, no DCX + cells were microscopically detectable in the DG. Representative micrographs from the 91- and 101-year-old cases are included to illustrate the DCX + neurons as examples (Fig. 9a–e; Suppl. Figure 4a–c).

In the sections passing the amygdala from the 91- and 101-year-old cases, a band of DCX + cells was still visible along the PLN (Fig. 9a, b; Suppl. Figure 4a). At higher magnifications, these DCX + cells showed light or strong immunoreactivity (Fig. 9b; Suppl. Figure 4c). Migratory cellular chains were still present in the PLN and neighboring areas. In the BM, some lightly stained cells were found, as were short migratory chains (Fig. 9c). In the neocortex and entorhinal cortex, DCX + neurons were still seen in layers I to III, while the vast majority of them were lightly to moderately stained (Fig. 9d, e; Suppl. Figure S4b).

Quantitative Analysis of DCX + Neurons in Selected Cerebral Regions

Cell count was carried out to verify the age-related decrease in DCX + neurons in selected neocortical areas, amygdala, and DG (Table 1) (Fig. 10a). Sections (2 sections/brain) passing the frontal, temporal, and occipital poles, respectively, were used for quantification of DCX + cells around layer II. We choose these areas in a consideration that the data obtained could reflect the scope of broadness in the regional distribution of cortical DCX + neurons in different age groups. Also, for a practical reason, the cell count workload could be minimized using these relatively small-sized polar cortex sections. DCX + neurons around the PLN of the amygdala and the SGZ of the DG were also counted, using sections approximately at the mid-amygdalar and mid-hippocampal levels (two sections/brain). It should be noted that a zero value was arbitrarily given in the cases that no DCX + neurons were found microscopically, to allow the statistical analyses between groups.

The numerical densities of DCX + neurons around layer II in the frontal pole neocortex were 52.1 ± 23.3, 23.4 ± 12.5, 0 ± 0, and 0 ± 0 cells/mm^2 (mean ± SD, same format below) in the infant/toddler, adolescent, adult, and aged groups (Fig. 10B). One-way ANOVA test showed an overall significant difference among the means ($P < 0.0001$, $F = 23.3$, DF = 3, 20), with intergroup difference reached for the infant and adolescent groups relative to other groups, respectively (Fig. 10b). The density of layer II DCX + neurons in the temporal pole neocortex were 91.6 ± 24.6, 53.6 ± 20.9, 44.6 ± 28.9, and 12.8 ± 4.6 cells/mm^2 in infant/toddler, adolescent, adult, and aged groups, which showed an overall as well as some intergroup differences ($P = 0.0001$, $F = 11.5$, DF = 3, 20) (Fig. 10c). The density of layer II DCX + neurons in the occipital pole neocortex were 35.8 ± 15.7, 10.3 ± 2.7, 0 ± 0, and 0 ± 0 cells/mm^2 in the above groups of the same listing order, showing significant age-related difference ($P = 0.0001$, $F = 25.1$, DF = 3, 20) (Fig. 10d). The numerical densities of DCX + amygdalar neurons around the PLN were 494.3 ± 198.1, 719.2 ± 123.8, 340.6 ± 197.3, and 234.5 ± 92.6 cells/mm^2 in the groups, showing significant age-related difference as indicated ($P < 0.0001$, $F = 15.0$, DF = 3, 21) (Fig. 10e). Finally, the estimated densities of DCX + neurons in the SGZ/GCL of the DG were 168.7 ± 107.4, 3.8 ± 6.6, 0 ± 0, and 0 ± 0 cells/mm^2 in the groups. There was a significant overall difference among the means ($P < 0.0001$, $F = 15.8$, DF = 3, 22), with the infant group significant different relative to other groups by post hoc test (Fig. 10f).

Schematic Presentation of the Topographic Evolution of DCX + Neurons with Age

To present a whole brain overview, we schematically summarized the trend of age-related changes in the distribution and amount of DCX + neurons in the cerebral cortex, amygdala, and DG, using four representative fronto-occipital planes, based on the microscopical assessments and the above cell counting data (Fig. 11). Thus, in the infant/toddler group (Fig. 11a), layer II DCX + neurons occurred throughout the cerebrum from the frontal to occipital pole, with the cells most densely present in the temporal lobe. DCX + amygdalar neurons were abundant, densely packed in the PLN but also occurred in other subnuclei. A significant population of DCX + immature granule cells were seen in the DG. In the adolescent group (Fig. 11b), DCX + neurons were detectable in the frontal, parietal, and occipital lobes and commonly seen over the temporal neocortex and entorhinal cortex. A large number of DCX + neurons resided in amygdala, also concentrating in the PLN and spreading into the central amygdalar regions. DCX + immature granule

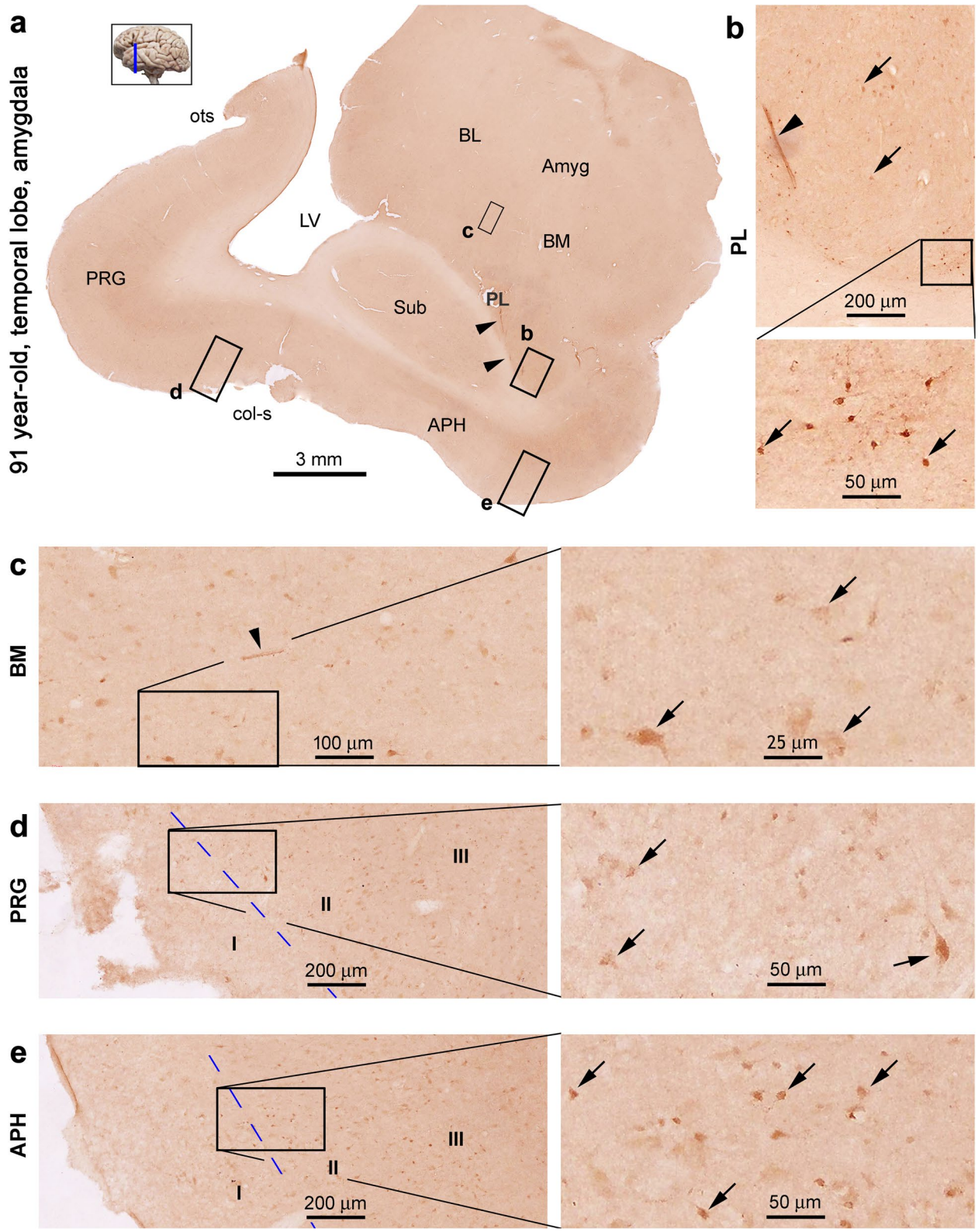

Fig. 9 DCX + neuronal profiles in the temporal lobe section at the level of the amygdala in the 91-year-old case. Panel arrangements, anatomical structures, and scale bars are as indicated. Labeled neuronal somata (as pointed with arrows) in the amygdala (**a**–**c**) and cortex (**a**, **d**, **e**) mostly exhibit light to moderate intensity. Strongly labeled cells together with migratory cellular chains remain in the paralaminar (PL) nucleus (**b**). Abbreviations are as defined in Figs. 1 and 2

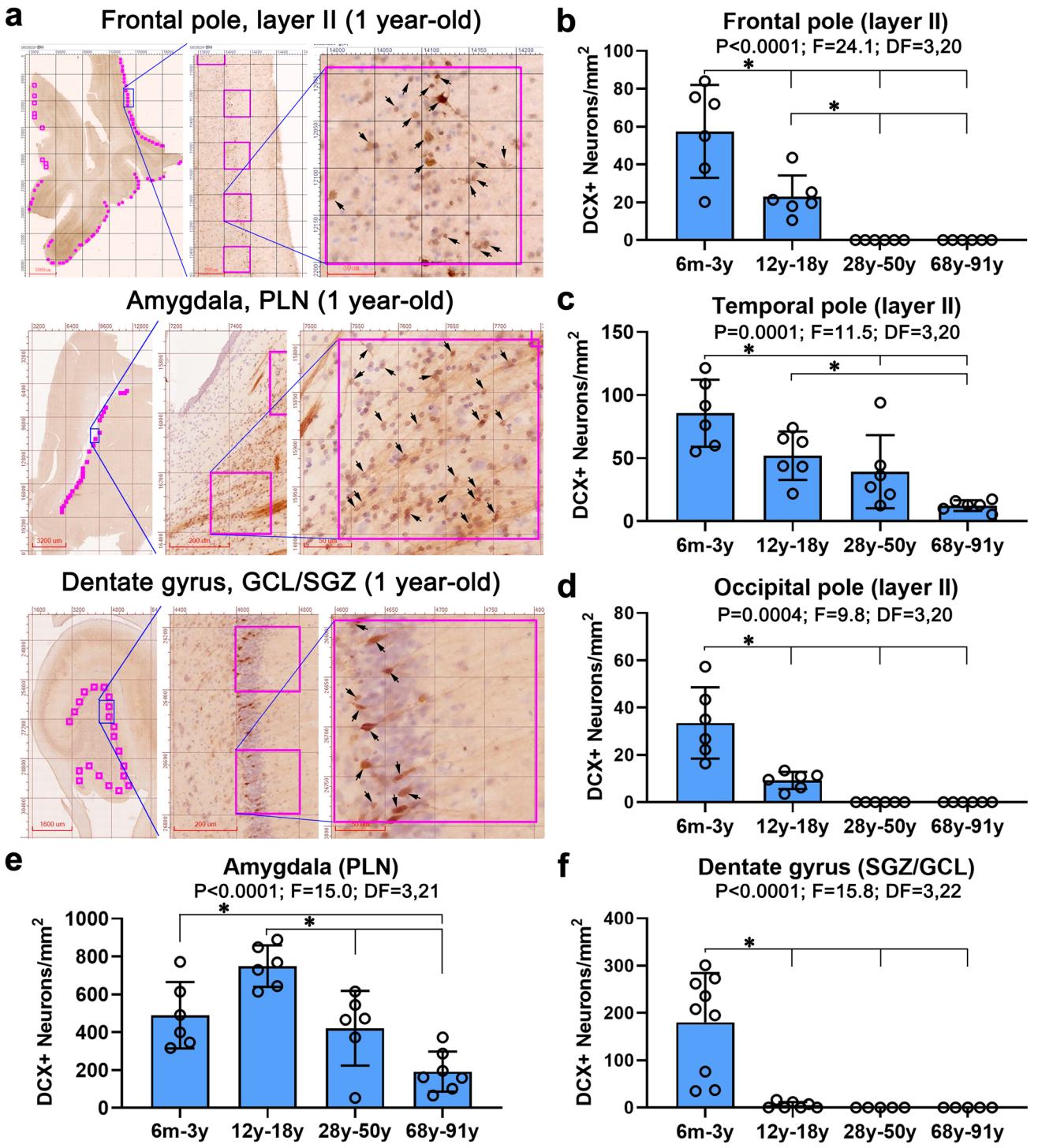

Fig. 10 Quantitative analyses of DCX + neurons in selective neocortical areas, amygdala, and dentate gyrus. **a** illustrates the methodology for cell count in randomly determined zones in 200 × 200 µm^2 size, using sections (counterstained with hematoxylin) from the 1-year-old case as examples. The counting zones are approximately centered over layer II, the paralaminar nucleus (PLN) of amygdala, and the subgranular zone (SGZ). The final density of the DCX + neurons calculated for a given area and case is based on cell count in two sections. The density values from individual cases in the age groups (indicates in Table 1) are graphed according to the regions analyzed, i.e., the frontal, temporal, and occipital polar neocortex, and the amygdala and DG, respectively (**b**–**f**). A zero value is given if no DCX + cells are clearly observed. Statistical results and significant intergroup differences (*) based on one-way ANOVA test with Bonferroni's pair-wise multiple comparisons are provided in graphs

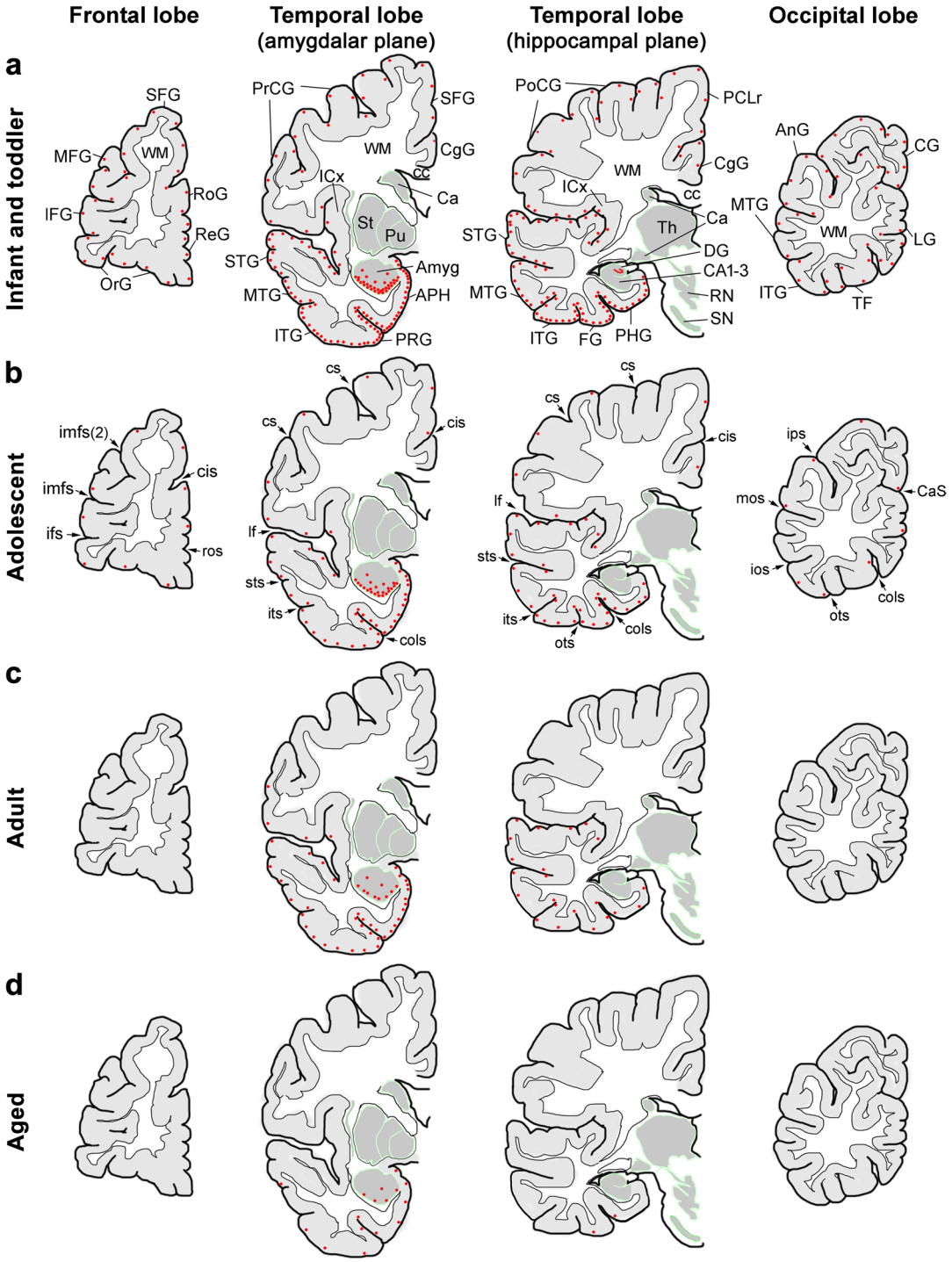

Fig. 11 Schematic illustration of age-related changes in the regional distribution and relative amount of DCX + neurons in the cerebral neocortex, amygdala, and dentate gyrus. The maps are based on the densitometric data and visual estimation through examination over the Motic-scanned images at low and high magnifications from multiple sections from individual brains. Red dots represent the relative amount of DCX + neurons and their locations at four representative fronto-occipital planes as indicated. DCX + neurons are most abundant in the infant/toddler group, which are present throughout the cerebral lobes, in the amygdala and the dentate gyrus (DG) (**a**). In the adolescent group (**b**), DCX + neurons are reduced in number but remain detectable across the cerebral lobes. The temporal lobe cortex and amygdala have the highest density of the labeled neurons, while those in the DG are occasionally found. In the adult group (**c**), DCX + neurons are detectable across the temporal lobe cortex and in the amygdala, but rarely seen in the DG. In the aged group (**d**), DCX + neurons are restricted to the temporal lobe cortex adjoining the amygdala wherein a substantial number of neurons remained. Abbreviations of neuroanatomical terms are as defined in Figs. 1 and 2

cells were occasionally detectable in the DG. In the adult group (Fig. 11c), DCX + cortical neurons were essentially disappeared over the frontal, parietal, and occipital regions, although they were still present across the temporal cortex. A fairly large number of DCX + neurons remained in the amygdala, whereas DCX + cells in the DG were essentially not detectable. In the aged group, DCX + neurons were restricted to the cortical area adjoining the amygdala wherein a substantial number of DCX + neurons remained, and again, no labeled cells in the DG (Fig. 11d).

Western Blotting of DCX Protein in the Temporal Neocortex and Amygdala

Since DCX + neurons existed in the temporal cortex and amygdala in all age groups, we carried out Western blotting using lysates from the frozen temporal lobe slices to verify an age-related decline in the levels of DCX protein. Samples were dissected out from the superficial part of the temporal neocortex, and the amygdalar area corresponding to the PLN. Lysates from cases in the adolescent ($n = 5$), adult ($n = 5$), and aged ($n = 6$) groups were immunoblotted (Table 1). Levels of DCX standardized to GAPDH were further normalized to the mean (defined as 100%) of the values of the cortical lysates of the adolescent group (Suppl. Figure 5a–d).

Compared to the adolescent group ($100.0 \pm 9.5\%$, mean ± S.D., same format below), levels of DCX protein in the temporal neocortical lysates were reduced to $35.6 \pm 18.3\%$ ($P < 0.05$) and $7.9 \pm 5.4\%$ ($P < 0.05$), respectively, in the adult and aged groups (one-way ANOVA with Bonferroni's multiple comparison test) (Suppl. Figure 5a, c, e). DCX levels in the amygdalar lysates in the adult and aged groups were reduced to $50.9 \pm 20.2\%$ ($P < 0.05$) and $17.2 \pm 12.7\%$ ($P < 0.05$), respectively, of the values ($100.0 \pm 18.9\%$) in the adolescents (Suppl. Figure 5b, c, e). Significant differences existed for DCX levels in the cortical lysates of the adolescent relative to the adult and aged groups ($P < 0.05$), and for DCX levels in the amygdalar lysates between each pair of the three age groups ($P < 0.05$), according to post hoc tests (Suppl. Figure 5e).

Discussion

This study was aimed to update the assessment of DCX + neurons in the human cerebral cortex and amygdala. We adjunctly examined the DCX + neurons in the DG, which is related to a debated issue whether specialized tissue fixation protocol is needed to detect DCX expression here relating to hippocampal neurogenesis [43, 54–62]. Impact of tissue processing factors including fixation always exist in postmortem human brain studies. Our multi-case and multi-region comparative analyses involved a principle of positive internal controls [60]. Since conventional formalin fixation was used in this study, we could not rule out a possibility that DCX immunolabeling was parallelly underestimated across brains and regions. With this point being considered, we discuss our results based on the observations de facto.

The current whole cerebrum mapping study updated the information regarding age-related changes in the population, regional distribution, and morphology of layer II and amygdalar DCX + neurons in the human brains. In general, the topographic distribution of the layer II DCX + neurons changes from occurring across the entire cerebrum to being restricted in the temporal cortex adjoining the amygdala, with the advance of age. The decrease in the overall population and regional distribution of the labeled neurons appear correlated, and are in line with the age-related decline in the levels of DCX protein detected by immunoblot analysis. In all brains examined, the DCX + neurons in a given cortical area and the amygdala composed of a cohort of morphologically heterogeneous neuronal cells, with some small-sized and morphologically primitive ones arranged in clusters and chains. This small-sized population was reduced in the adult and aged cases relative to the infant/toddler and adolescent cases. Specifically, the DCX + chain-like structures were more frequently seen, involved more cells and extended longer in distance in the cortex and amygdala in the infant/toddler and adolescent relative to the adult and aged cases. Our data support the notion that DCX + cells in the human cerebral cortex and amygdalar are a population of immature neurons [1–4, 13, 14, 43, 63]. The small-sized ones are primitive, appear to migrate away from the clusters and chains, grow their soma, and become the larger and mature-looking subpopulation.

The origin and neuronal phenotype fate of layer II and amygdalar DCX + neurons remain an issue to be reconciled. Layer II DCX + neurons in the rodent piriform cortex and human temporal neocortex were found to co-express the embryonically pallidum-derived excitatory neuronal lineage markers the transcription factors T-box brain 1 (TBR1) and the cut like homeobox 1, but were not colocalized with GABAergic markers [44, 61]. Another study also showed TBR1 colocalization in layer II DCX + neurons in mouse, guinea pig, and rabbit cerebral cortex, while some faintly stained DCX + neurons were noted to express the subpallial lineage transcriptive factor distalless [15]. DCX + neurons in the human amygdala were reported to co-express mainly TBR1, and to a lesser extent, the chicken ovalbumin upstream promoter transcription factor II, also a subpallial interneuron lineage marker [23]. Other previous studies reported the colocalization of layer II DCX + neurons with GABAergic markers in guinea

pigs, cats, monkeys, and humans [13, 14, 43, 46, 47]. In addition, tangential DCX + migratory chains have been reported in the white matter in infant human, porcine, and ferret cerebral cortex [46, 47, 64, 65]. In this study, we also observed such tangential migratory chains located between the amygdala and temporal cortex in the infant cases. An intriguing phenomenon is that the DCX + neurons around the superficial cortical layers can form migratory chains running tangentially in layer I and "waterfall-like" migratory clusters extending from this layer into deeper layers in the cat, monkey, and human cerebral cortex over a wide age range, even in some old macaques [14, 16]. This observation appears in congruent with the pattern of interneuron migration using the marginal zone (lately layer I) as the transit route, which might persist into postnatal life possibly because cortical expansion (e.g., the grey matter folding) is much greater on the pial than the what matter side in gyrified brains [63–65].

The functional implication of cortical layer II and amygdalar DCX + neurons has been recently elaborated in perspective of cerebral development and evolution [3–5, 66]. It is considered that these DCX + immature neurons contribute to a protracted neuronal development important for modulation of cognitive functions and emotional behaviors from infancy to adulthood. In support of the above view, the present study showed the presence of layer II DCX + neurons across much of cerebral regions from infancy to adolescence, and a persistency of these neurons in the temporal cortex and amygdala into old ages. Many neurological and psychiatric diseases such as febrile seizures, autism, epilepsy, attention and mode disorders, and schizophrenia have been related to aberrant neuronal development and imbalanced excitatory and inhibitory circuitries [67–72]. In this regard, it would be important to clarify whether the cortical and amygdalar DCX + immature neurons may mature into excitatory or inhibitory neurons, or actually both types, in the future.

An inherent issue in regard to postmortem human brain study involves the effect of antemortem conditions on the observation and interpretation of neuronal measurements obtained experimentally. It is particularly difficult to appraise whether, and if so, to what extent, various peripheral or systematic diseases or conditions would impact the neuroanatomical and/or neurochemical data obtained from postmortem brain samples. It is even more so when a study involves the analysis of brains from infant, childhood, and young adult individuals, whose deaths are always caused by some fatal diseases such as malignant tumors, with the patients subjected to intensive antemortem medical attention or complex complications. Nonetheless, the fact that DCX + immature neurons are still observed in the cerebral cortex and amygdala in postmortem brains of even these severely diseased patients would likely strengthen the point that these neurons must exist substantially under physiological conditions and play some fundamental biological roles. Further worth noting, in the present study several cases in the aged group showed various extents of cerebral β-amyloid (Aβ) and tau pathologies (Table 1). DCX + neurons were persistent in the temporal cortex and amygdala in these brains. A previous study also reported the coexistence of DCX + neurons with Aβ plaques in the neocortex in aged monkeys [16]. However, we have not systematically explored if AD-type neuropathology would affect DCX + immature neurons.

In summary, DCX + neurons exist in human cerebral cortex and amygdala essentially lifelong. The topographic distribution of layer II DCX + neurons changes from being present across the cerebrum to being restricted in the temporal cortex adjoining the amygdala with age. Our findings are consistent with the notion that DCX + immature neurons serve as an important cellular substrate to support neuronal network plasticity, which can occur broadly in human cerebrum but also evolve during life in an age/region-related manner.

Supplementary Information The online version contains supplementary material available at https://doi.org/10.1007/s12035-023-03261-7.

Acknowledgements We would like to express our greatest gratitude and respect to the individuals who donate their brains to help understand human brain health and diseases.

Author Contribution Conceptualization, Lily Wan, Aihua Pan, and Xiao-Xin Yan. Data curation, Ya-Nan Li and Dan-Dan Hu. Funding acquisition, Lily-Wan, Ewen Tu, Xiao-Sheng Wang, Hui Wang, Xiao-Ping Wang, and Xiao-Xin Yan. Methodology, Ya-Nan Li, Dan-Dan Hu, Xiao-Lu Cai, Yan Wang, Chen Yang, Juan Jiang, Qi-Lei Zhang, Tian Tu. Writing—original draft, Lily Wan. Writing—review and editing, Aihua Pan and Xiao-Xin Yan.

Funding This study was supported by National Natural Science Foundation of China (#82071223), Ministry of Science and Technology of China (STI2030-Major Projects#2021ZD0201103 and #2021ZD0201803), and Hunan Provincial Science and Technology Foundation (#2018JJ2552 and #2022JJ40817).

Data Availability All data needed to evaluate the conclusions in the paper are present in the paper and/or the supplemental data. Upon reasonable request, additional experimental data and materials for this study can be requested at the discretion of the corresponding author.

Declarations

Ethics Approval and Consent to Participate The use of postmodern human brains was approved by the Ethics Committee for Research and Education at Xiangya School of Medicine, in compliance with the Code of Ethics of the World Medical Association (Declaration of Helsinki). Written informed consent for body/brain donation was obtained by the willed body donation center of Xiangya School of Medicine.

Consent for Publication Not applicable.

Competing interests The authors declare no competing interests.

References

1. Bonfanti L, Nacher J (2012) New scenarios for neuronal structural plasticity in non-neurogenic brain parenchyma: the case of cortical layer II immature neurons. Prog Neurobiol 98(1):1–15
2. La Rosa C, Parolisi R, Bonfanti L (2020) Brain structural plasticity: from adult neurogenesis to immature neurons. Front Neurosci 14:75
3. Kim JY, Paredes MF (2021) Implications of extended inhibitory neuron development. Int J Mol Sci 22(10):5113
4. Bonfanti L, Seki T (2021) The PSA-NCAM-positive "immature" neurons: an old discovery providing new vistas on brain structural plasticity. Cells 10(10):2542
5. Seki T, Arai Y (1991) Expression of highly polysialylated NCAM in the neocortex and piriform cortex of the developing and the adult rat. Anat Embryol (Berl) 184(4):395–401
6. Bonfanti L, Olive S, Poulain DA, Theodosis DT (1992) Mapping of the distribution of polysialylated neural cell adhesion molecule throughout the central nervous system of the adult rat: an immunohistochemical study. Neuroscience 49(2):419–436
7. Bernier PJ, Parent A (1998) Bcl-2 protein as a marker of neuronal immaturity in postnatal primate brain. J Neurosci 18(7):2486–2497
8. Fox GB, Fichera G, Barry T, O'Connell AW, Gallagher HC, Murphy KJ, Regan CM (2000) Consolidation of passive avoidance learning is associated with transient increases of polysialylated neurons in layer II of the rat medial temporal cortex. J Neurobiol 45(3):135–141
9. Nacher J, Crespo C, McEwen BS (2001) Doublecortin expression in the adult rat telencephalon. Eur J Neurosci 14(4):629–644
10. Bernier PJ, Bedard A, Vinet J, Levesque M, Parent A (2002) Newly generated neurons in the amygdala and adjoining cortex of adult primates. Proc Natl Acad Sci U S A 99(17):11464–11469
11. Fudge JL (2004) Bcl-2 immunoreactive neurons are differentially distributed in subregions of the amygdala and hippocampus of the adult macaque. Neuroscience 127(2):539–556
12. Fudge JL, deCampo DM, Becoats KT (2012) Revisiting the hippocampal-amygdala pathway in primates: association with immature-appearing neurons. Neuroscience 212:104–119
13. Xiong K, Luo DW, Patrylo PR, Luo XG, Struble RG, Clough RW, Yan XX (2008) Doublecortin-expressing cells are present in layer II across the adult guinea pig cerebral cortex: partial colocalization with mature interneuron markers. Exp Neurol 211(1):271–282
14. Cai Y, Xiong K, Chu Y, Luo DW, Luo XG, Yuan XY, Struble RG, Clough RW et al (2009) Doublecortin expression in adult cat and primate cerebral cortex relates to immature neurons that develop into GABAergic subgroups. Exp Neurol 216(2):342–356
15. Luzzati F, Bonfanti L, Fasolo A, Peretto P (2009) DCX and PSA-NCAM expression identifies a population of neurons preferentially distributed in associative areas of different pallial derivatives and vertebrate species. Cereb Cortex 19(5):1028–1041
16. Zhang XM, Cai Y, Chu Y, Chen EY, Feng JC, Luo XG, Xiong K, Struble RG et al (2009) Doublecortin-expressing cells persist in the associative cerebral cortex and amygdala in aged nonhuman primates. Front Neuroanat 3:17
17. Marlatt MW, Philippens I, Manders E, Czéh B, Joels M, Krugers H, Lucassen PJ (2011) Distinct structural plasticity in the hippocampus and amygdala of the middle-aged common marmoset (Callithrix jacchus). Exp Neurol 230(2):291–301
18. De Nevi E, Marco-Salazar P, Fondevila D, Blasco E, Pérez L, Pumarola M (2013) Immunohistochemical study of doublecortin and nucleostemin in canine brain. Eur J Histochem 57(1):e9
19. Martí-Mengual U, Varea E, Crespo C, Blasco-Ibáñez JM, Nacher J (2013) Cells expressing markers of immature neurons in the amygdala of adult humans. Eur J Neurosci 37(1):10–22
20. Patzke N, LeRoy A, Ngubane NW, Bennett NC, Medger K, Gravett N, Kaswera-Kyamakya C, Gilissen E et al (2014) The distribution of doublecortin-immunopositive cells in the brains of four afrotherian mammals: the Hottentot golden mole (Amblysomus hottentotus), the rock hyrax (Procavia capensis), the eastern rock sengi (Elephantulus myurus) and the four-toed sengi (Petrodromus tetradactylus). Brain Behav Evol 84(3):227–241
21. Liu YW, Curtis MA, Gibbons HM, Mee EW, Bergin PS, Teoh HH, Connor B, Dragunow M et al (2008) Doublecortin expression in the normal and epileptic adult human brain. Eur J Neurosci 28(11):2254–2265
22. Piumatti M, Palazzo O, La Rosa C, Crociara P, Parolisi R, Luzzati F, Lévy F, Bonfanti L (2018) Non-newly generated, "immature" neurons in the sheep brain are not restricted to cerebral cortex. J Neurosci 38(4):826–842
23. Sorrells SF, Paredes MF, Velmeshev D, Herranz-Pérez V, Sandoval K, Mayer S, Chang EF, Insausti R et al (2019) Immature excitatory neurons develop during adolescence in the human amygdala. Nat Commun 10(1):2748
24. Ai JQ, Luo R, Tu T, Yang C, Jiang J, Zhang B, Bi R, Tu E et al (2021) Doublecortin-expressing neurons in Chinese tree shrew forebrain exhibit mixed rodent and primate-like topographic characteristics. Front Neuroanat 15:727883
25. van Groen T, Kadish I, Popović N, Caballero Bleda M, Baño-Otalora B, Rol MA, Madrid JA, Popović M (2021) Widespread doublecortin expression in the cerebral cortex of the Octodon degus. Front Neuroanat 15:656882
26. Chawana R, Patzke N, Alagaili AN, Bennett NC, Mohammed OB, Kaswera-Kyamakya C, Gilissen E, Ihunwo AO et al (2016) The distribution of Ki-67 and doublecortin immunopositive cells in the brains of three Microchiropteran species, Hipposideros fuliginosus, Triaenops persicus, and Asellia tridens. Anat Rec (Hoboken) 299(11):1548–1560
27. Fasemore TM, Patzke N, Kaswera-Kyamakya C, Gilissen E, Manger PR, Ihunwo AO (2018) The distribution of Ki-67 and doublecortin-immunopositive cells in the brains of three Strepsirrhine Primates: Galago demidoff, Perodicticus potto, and Lemur catta. Neuroscience 372:46–57
28. La Rosa C, Cavallo F, Pecora A, Chincarini M, Ala U, Faulkes CG, Nacher J, Cozzi B, et al. (2020) Phylogenetic variation in cortical layer II immature neuron reservoir of mammals. Elife 9
29. Rotheneichner P, Belles M, Benedetti B, König R, Dannehl D, Kreutzer C, Zaunmair P, Engelhardt M et al (2018) Cellular plasticity in the adult murine piriform cortex: continuous maturation of dormant precursors into excitatory neurons. Cereb Cortex 28(7):2610–2621
30. Benedetti B, Dannehl D, König R, Coviello S, Kreutzer C, Zaunmair P, Jakubecova D, Weiger TM et al (2020) functional integration of neuronal precursors in the adult murine piriform cortex. Cereb Cortex 30(3):1499–1515
31. Xiong K, Cai Y, Zhang XM, Huang JF, Liu ZY, Fu GM, Feng JC, Clough RW et al (2010) Layer I as a putative neurogenic niche in young adult guinea pig cerebrum. Mol Cell Neurosci 45(2):180–191
32. He X, Zhang XM, Wu J, Fu J, Mou L, Lu DH, Cai Y, Luo XG et al (2014) Olfactory experience modulates immature neuron development in postnatal and adult guinea pig piriform cortex. Neuroscience 259:101–112
33. Rossi SL, Mahairaki V, Zhou L, Song Y, Koliatsos VE (2014) Remodeling of the piriform cortex after lesion in adult rodents. NeuroReport 25(13):1006–1012

34. Srikandarajah N, Martinian L, Sisodiya SM, Squier W, Blumcke I, Aronica E, Thom M (2009) Doublecortin expression in focal cortical dysplasia in epilepsy. Epilepsia 50(12):2619–2628
35. Sakurai M, Suzuki H, Tomita N, Sunden Y, Shimada A, Miyata H, Morita T (2018) Enhanced neurogenesis and possible synaptic reorganization in the piriform cortex of adult rat following kainic acid-induced status epilepticus. Neuropathology 38(2):135–143
36. Nordahl CW, Scholz R, Yang X, Buonocore MH, Simon T, Rogers S, Amaral DG (2012) Increased rate of amygdala growth in children aged 2 to 4 years with autism spectrum disorders: a longitudinal study. Arch Gen Psychiatry 69(1):53–61
37. Maheu ME, Davoli MA, Turecki G, Mechawar N (2013) Amygdalar expression of proteins associated with neuroplasticity in major depression and suicide. J Psychiatr Res 47(3):384–390
38. Avino TA, Barger N, Vargas MV, Carlson EL, Amaral DG, Bauman MD, Schumann CM (2018) Neuron numbers increase in the human amygdala from birth to adulthood, but not in autism. Proc Natl Acad Sci U S A 115(14):3710–3715
39. Schumann CM, Scott JA, Lee A, Bauman MD, Amaral DG (2019) Amygdala growth from youth to adulthood in the macaque monkey. J Comp Neurol 527(18):3034–3045
40. Mikkonen M, Soininen H, Kälviänen R, Tapiola T, Ylinen A, Vapalahti M, Paljärvi L, Pitkänen A (1998) Remodeling of neuronal circuitries in human temporal lobe epilepsy: increased expression of highly polysialylated neural cell adhesion molecule in the hippocampus and the entorhinal cortex. Ann Neurol 44(6):923–934
41. Chareyron LJ, Amaral DG, Lavenex P (2016) Selective lesion of the hippocampus increases the differentiation of immature neurons in the monkey amygdala. Proc Natl Acad Sci U S A 113(50):14420–14425
42. Yachnis AT, Roper SN, Love A, Fancey JT, Muir D (2000) Bcl-2 immunoreactive cells with immature neuronal phenotype exist in the nonepileptic adult human brain. J Neuropathol Exp Neurol 59(2):113–119
43. Franjic D, Skarica M, Ma S, Arellano JI, Tebbenkamp ATN, Choi J, Xu C, Li Q et al (2022) Transcriptomic taxonomy and neurogenic trajectories of adult human, macaque, and pig hippocampal and entorhinal cells. Neuron 110(3):452-469.e414
44. Coviello S, Gramuntell Y, Klimczak P, Varea E, Blasco-Ibañez JM, Crespo C, Gutierrez A, Nacher J (2022) Phenotype and distribution of immature neurons in the human cerebral cortex layer II. Front Neuroanat 16:851432
45. Sanai N, Nguyen T, Ihrie RA, Mirzadeh Z, Tsai HH, Wong M, Gupta N, Berger MS et al (2011) Corridors of migrating neurons in the human brain and their decline during infancy. Nature 478(7369):382–386
46. Paredes MF, James D, Gil-Perotin S, Kim H, Cotter JA, Ng C, Sandoval K, Rowitch DH et al (2016) Extensive migration of young neurons into the infant human frontal lobe. Science 354(6308):aaf7073
47. Nascimento MA, Biagiotti S, Herranz-Pérez V, Bueno R, Ye JY, Abel T, Rubio-Moll JS, Garcia-Verdugo JM et al (2022) Persistent postnatal migration of interneurons into the human entorhinal cortex. bioRxiv. https://doi.org/10.1101/2022.03.19.484996
48. Yan XX, Ma C, Bao AM, Wang XM, Gai WP (2015) Brain banking as a cornerstone of neuroscience in China. Lancet Neurol 14(2):136
49. Ma C, Bao AM, Yan XX, Swaab DF (2019) Progress in human brain banking in China. Neurosci Bull 35(2):179–182
50. Qiu W, Zhang H, Bao A, Zhu K, Huang Y, Yan X, Zhang J, Zhong C et al (2019) Standardized Operational Protocol for Human Brain Banking in China. Neurosci Bull 35(2):270–276
51. Hu X, Hu ZL, Li Z, Ruan CS, Qiu WY, Pan A, Li CQ, Cai Y et al (2017) Sortilin fragments deposit at senile plaques in human cerebrum. Front Neuroanat 11:45
52. Tu T, Jiang J, Zhang QL, Wan L, Li YN, Pan A, Manavis J, Yan XX (2020) extracellular sortilin proteopathy relative to β-amyloid and tau in aged and Alzheimer's disease human brains. Front Aging Neurosci 12:93
53. Jiang J, Yang C, Ai JQ, Zhang QL, Cai XL, Tu T, Wan L, Wang XS et al (2022) Intraneuronal sortilin aggregation relative to granulovacuolar degeneration, tau pathogenesis and sorfra plaque formation in human hippocampal formation. Front Aging Neurosci 14:926904
54. Sorrells SF, Paredes MF, Cebrian-Silla A, Sandoval K, Qi D, Kelley KW, James D, Mayer S et al (2018) Human hippocampal neurogenesis drops sharply in children to undetectable levels in adults. Nature 555(7696):377–381
55. Moreno-Jiménez EP, Flor-García M, Terreros-Roncal J, Rábano A, Cafini F, Pallas-Bazarra N, Ávila J, Llorens-Martín M (2019) Adult hippocampal neurogenesis is abundant in neurologically healthy subjects and drops sharply in patients with Alzheimer's disease. Nat Med 25(4):554–560
56. Flor-García M, Terreros-Roncal J, Moreno-Jiménez EP, Ávila J, Rábano A, Llorens-Martín M (2020) Unraveling human adult hippocampal neurogenesis. Nat Protoc 15(2):668–693
57. Terreros-Roncal J, Moreno-Jiménez EP, Flor-García M, Rodríguez-Moreno CB, Trinchero MF, Cafini F, Rábano A, Llorens-Martín M (2021) Impact of neurodegenerative diseases on human adult hippocampal neurogenesis. Science 374(6571):1106–1113
58 Arellano JI, Duque A, Rakic P (2022) Comment on "Impact of neurodegenerative diseases on human adult hippocampal neurogenesis." Science 376(6590):eabn7083
59. Alvarez-Buylla A, Cebrian-Silla A, Sorrells SF, Nascimento MA, Paredes MF, Garcia-Verdugo JM, Yang Z, Huang EJ (2022) Comment on "Impact of neurodegenerative diseases on human adult hippocampal neurogenesis." Science 376(6590):eabn8861
60. Sorrells SF, Paredes MF, Zhang Z, Kang G, Pastor-Alonso O, Biagiotti S, Page CE, Sandoval K et al (2021) Positive controls in adults and children support that very few, if any, new neurons are born in the adult human hippocampus. J Neurosci 41(12):2554–2565
61. Gómez-Climent MA, Castillo-Gómez E, Varea E, Guirado R, Blasco-Ibáñez JM, Crespo C, Martínez-Guijarro FJ, Nácher J (2008) A population of prenatally generated cells in the rat paleocortex maintains an immature neuronal phenotype into adulthood. Cereb Cortex 18(10):2229–2240
62. Brown JP, Couillard-Després S, Cooper-Kuhn CM, Winkler J, Aigner L, Kuhn HG (2003) Transient expression of doublecortin during adult neurogenesis. J Comp Neurol 467(1):1–10
63. Llorca A, Deogracias R (2022) Origin, development, and synaptogenesis of cortical interneurons. Front Neurosci 16:929469
64. Ellis JK, Sorrells SF, Mikhailova S, Chavali M, Chang S, Sabeur K, McQuillen P, Rowitch DH (2019) Ferret brain possesses young interneuron collections equivalent to human postnatal migratory streams. J Comp Neurol 527(17):2843–2859
65. Porter DDL, Henry SN, Ahmed S, Rizzo AL, Makhlouf R, Gregg C, Morton PD (2022) Neuroblast migration along cellular substrates in the developing porcine brain. Stem Cell Reports 17(9):2097–2110
66. Page CE, Biagiotti SW, Alderman PJ, Sorrells SF (2022) Immature excitatory neurons in the amygdala come of age during puberty. Dev Cogn Neurosci 56:101133
67. Ajram LA, Horder J, Mendez MA, Galanopoulos A, Brennan LP, Wichers RH, Robertson DM, Murphy CM et al (2017) Shifting brain inhibitory balance and connectivity of the prefrontal cortex of adults with autism spectrum disorder. Transl Psychiatry 7(5):e1137

68. Mosili P, Maikoo S, Mabandla MV, Qulu L (2020) The pathogenesis of fever-induced febrile seizures and its current state. Neurosci Insights 15:2633105520956973
69. Dóra F, Renner É, Keller D, Palkovits M, Dobolyi Á (2022) Transcriptome profiling of the dorsomedial prefrontal cortex in suicide victims. Int J Mol Sci 23(13):7067
70. Howes OD, Shatalina E (2022) Integrating the neurodevelopmental and dopamine hypotheses of schizophrenia and the role of cortical excitation-inhibition balance. Biol Psychiatry 92(6):501–513
71. Lado WE, Xu X, Hablitz JJ (2022) Modulation of epileptiform activity by three subgroups of GABAergic interneurons in mouse somatosensory cortex. Epilepsy Res 183:106937
72. Yao HK, Guet-McCreight A, Mazza F, Moradi Chameh H, Prevot TD, Griffiths JD, Tripathy SJ, Valiante TA et al (2022) Reduced inhibition in depression impairs stimulus processing in human cortical microcircuits. Cell Rep 38(2):110232